Impact of ex-situ annealing on strain and composition of MBE grown GeSn

To cite this article before publication: Hui Jia *et al* 2020 *J. Phys. D: Appl. Phys.* in press https://doi.org/10.1088/1361-6463/abae94

IOP Publishing Journal Title
Journal **XX** (XXXX) XXXXXX https://doi.org/XXXX/XXXX

Impact of ex-situ annealing on strain and composition of MBE grown GeSn

Hui Jia[1], Pamela Jurczak[1], Junjie Yang[1], Mingchu Tang[1], Keshuang Li[1], Huiwen Deng[1], Manyu Dang[1], Siming Chen[1], Huiyun Liu[1]

[1] Department of Electronic and Electrical Engineering, University College London, Torrington Place, London, WC1E 7JE, UK

E-mail: hui.jia@ucl.ac.uk; pamela.jurczak@ucl.ac.uk

Received xxxxxx
Accepted for publication xxxxxx
Published xxxxxx

Abstract

The application of GeSn is extended to semiconductor lasers thanks to its band engineering via Sn composition and strain manipulation. As one of the strain engineering methods, thermal annealing, however, is not yet being widely adopted by the majority due to the thermal instability it induces. The thermal stability of GeSn is highly sensitive to initial material conditions, consequently thorough investigations are still demanded with different purposes. A detailed investigation on the thermal annealing effects of thick GeSn layers with a nominal 8% Sn grown on Ge-buffered Si (001) substrate by Molecular Beam Epitaxy (MBE) is presented here. Atomic force microscopy (AFM) and high-resolution x-ray diffraction (HRXRD) were used to trace the change of GeSn surface morphology and the strain relaxation after annealing. It is confirmed that the tetragonal compressive strain in GeSn, which is a proven detriment to the realisation of direct-bandgap material, can be relaxed by 90% while improving crystal quality, e.g. reduced surface roughness by appropriate annealing conditions. These findings reveal the potential of annealed GeSn to serve as a much thinner (750 nm), better lattice-matched to GeSn active layer and highly strain-relaxed platform to grow GeSn on compared to the thick Ge or the compositional-graded (Si)GeSn buffer layers, which are complicated and time-consuming in growth procedures and also securing an easier approach.

Keywords: GeSn buffer, annealing, MBE

1. Introduction

GeSn alloy has received considerable attention in recent years as it overcomes the indirect-bandgap nature of group-IV materials, rendering all-group-IV optoelectronic devices possible, which potentially enable the scalability of the fabrication of group-IV photonic integrated circuits with low cost and can be used for extremely high throughput data centres. The successful indirect-to-direct bandgap transformation of GeSn depends mainly on Sn composition and strain engineering. The direct character of the GeSn bandgap grows continuously with increasing Sn composition due to the Sn-induced conduction band mixing effect [1] while a direct-to-indirect bandgap crossover is shown to happen with around 8% Sn [2]. Earlier studies, therefore, made great efforts to grow crystalline GeSn with high Sn content up to approximately 30% [3, 4]. However, as the lattice mismatch between α-Sn (6.46 Å [5]) and Ge is large (14.2%), GeSn with 8% Sn will introduce a lattice mismatch of 1.1% to Ge and 5.3% to Si. Because of the greater lattice mismatch between GeSn and the underlying Ge/Si introduced by more Sn incorporation, crystal quality will degrade as the lattice mismatch induces increased misfit dislocations. Moreover, this measure imposes more compressive strain to GeSn, which

is proven to cancel the Γ-valley shrinkage effect by alloying with Sn [6, 7], and also limits Sn incorporation to Ge lattice sites [8]. Tensile strain, on the contrary, helps to increase the direct character of the GeSn bandgap beneficial to light emission without affecting crystal quality. Research focuses were then diverted to the strain engineering of the epitaxial GeSn. For example, thick GeSn layers demonstrated positive effects of accommodating tetragonal compressive strain by the generation of a point-defect-aided misfit dislocation network at the GeSn/Ge interface [6]. As the dislocations were trapped at the interface, bulk GeSn showed improved crystal quality. Other examples such as applying graded (Si)GeSn buffer layer [9-11], fabricating tensor arms [12], and depositing stressors and structuring microdisks [7, 13, 14], all contribute to the tailoring of GeSn bandgap and pushing the performance of the GeSn lasers towards room temperature operation and lower threshold operating power. Recent progress has shown that a tensile strain of 1.4% induced by all-around SiN_x stressors can turn GeSn into a direct-bandgap material with Sn composition as low as 5.4% [14]. Maximising the benefit of high-Sn-content-induced direct-bandgap character while obtaining improved crystal quality is consequently of paramount pursuit of researches related to GeSn-based laser devices.

Thermal annealing, as a widely used approach for strain relaxation, is usually unfavoured for GeSn because of the low solubility of Sn in Ge. After reaching certain critical annealing temperature, Sn segregation phenomenon arises, where Sn clusters deposit at the GeSn surface, at the GeSn/Ge interface or in bulk. It causes dramatically increased surface roughness, reduced lattice parameters and significantly varied surface morphology. Out of consideration for thermal processing during device fabrication, the thermal stability of GeSn has been investigated by a few tens of researches. The thermal budget for GeSn depends heavily on Sn composition, strain state within epilayer and growth conditions [15, 16]. For higher Sn content GeSn epitaxial growth on Ge/Si where the lattice mismatch is large, Sn segregation happens at lower annealing temperature as the strain needs to be released either through the generation of misfit dislocations or Sn out-diffusion [16]. Moreover, misfit and threading dislocations are proved to accelerate Sn diffusion, thus thick pre-relaxed GeSn layers can sustain higher temperature annealing than pseudomorphically grown layers but with a sharp transition from a high Sn-content alloy to a stable 1% Sn alloy [16]. Additionally, low-temperature-growth-induced point defects also affect the behaviour of Sn clusters formation, as they aid the lateral propagation of misfit dislocations and help to bind Sn atoms, reducing the strain in GeSn epilayers or local strain around Sn atoms [17]. The positive effects of thermal annealing include improved strain relaxation and crystal quality [6, 15, 18-25]. However, as the thermal annealing effects are highly sensitive to initial material conditions, i.e. the results can vary significantly with different material parameters, thorough investigations are still demanded for researches with different purposes.

Inspired by the benefits of thermal annealing in strain relaxation and crystal quality improvement, here we present investigations on ex-situ thermal annealing of 500 nm GeSn grown on 250 nm Ge based on Si (100) substrate by MBE designed to serve as a buffer for subsequent GeSn growth for optoelectronic devices. Indeed, the subsequently grown GeSn layer is expected to contain large Sn composition with little compressive strain, which is highly beneficial for the obtainment of the high directness of the bandgap. As the built-in compressive strain is an important parameter affecting GeSn crystal structure, this research examines the strain state of the GeSn epilayer after thermal annealing by various methods. It aims at finding appropriate annealing conditions to ensure maximum extent of strain relaxation while avoiding Sn segregation. The annealed GeSn layers can potentially provide a highly relaxed, lattice-matched buffer to the active layer. Moreover, a much thinner platform compared with a thick Ge or compositional-graded (Si)GeSn buffer with several microns thickness can be secured.

2. Experiment

As the goal is to grow a high-crystal-quality relaxed buffer for GeSn optoelectronic devices, pre-relaxed GeSn layers were chosen to provide better thermal stability and a Sn composition around GeSn bandgap indirect-to-direct crossover was selected to ensure better lattice match. 500 nm GeSn with a nominal Sn content of 8% was grown on 250 nm Ge buffer on Si (100) substrate by Veeco Gen 930 solid source MBE at a temperature window of 130-150 °C. 130 °C was the target growth temperature, however, due to the heating from the source effusion cells, there was an unintended temperature fluctuation between 130 and 150 °C during growth.The Ge buffer growth was performed following our previously optimised growth conditions [26]. A 5 nm Ge cap was deposited at the top of GeSn layer to prevent Sn segregation on the surface. After the growth, the samples were cleaved into 8 identical pieces and annealed at temperatures between 300 and 600 °C at step intervals of 50 °C for 5 minutes each in nitrogen ambient conditions in a Solaris 150 Rapid Thermal Processor. AFM was performed to probe surface morphology. The results of HRXRD (004) symmetric scan and reciprocal space maps (RSMs) were analysed and compared for lattice parameters and strain relaxation calculation. HRXRD investigation was performed in room temperature with a Jordan Valley Bede D1 x-ray diffractometer equipped with a Cu K_α source and detected by a YAP : Ce scintillator. The wavelength of the x-ray was 1.5406Å. RSMs were generated by collecting omega-2theta scans at different omega offsets (0.2º in total, with a step of 0.02º).

3. Results and discussion

3.1 Surface morphology

10 ×10 μm^2 AFM images of 500 nm GeSn/Ge/Si as-grown and after annealing at different temperatures (300 to 600 ℃) are shown in Figure 1(a-h), respectively. The surface of the as-grown GeSn sample undulates with randomly oriented hills and pits decorated with numerous tiny white spots, as can be seen in Figure 1(a). It has a root-mean-square (rms) roughness of 2.60 nm, which is smooth for a 500 nm thick GeSn layer with nominal 8% Sn as the surface roughness grows with GeSn layer thickness and Sn composition [6, 27-28].The tiny white dots were considered to be two possibilities. One is Sn precipitates because of the metastability of GeSn leading to phase separation of the Sn. There are two different phases of solid Sn precipitates: semiconductor phase α-Sn with diamond structure and metallic phase β-Sn with body-centred tetragonal unit cell [29]. The eutectic point of the GeSn alloy is 232 °C and the allotropic phase transition between α- and β-Sn is 13.5 °C. α-Sn is stable below the allotropic phase transition temperature while β-Sn phase is stable above this point [30]. Except for temperature, the formation and stability of the two phases of Sn crystallites depend heavily on pressure and interface effects [29]. For example, the temperature for the transformation from α-Sn to β-Sn can be elevated by the tensile strain in the precipitates to as high as around 200 °C in $Si_{0.95}Sn_{0.05}$ [30]. In our experiment, the growth temperature is low enough to suppress the Sn segregation, however, during the kinetic epitaxial growth process, Sn atoms may suffer from large compressive strain due to the significantly larger crystal lattice. Then the compressive strain can make the α-Sn to β-Sn transformation happen at decreased temperature, the more dense β-Sn phase thus forms clusters and diffuse to the surface, so we can even observe the white dots in the as-grown sample. Another possibility is Sn-induced surface roughening. There are two primary mechanisms controlling the surface morphology of epitaxial growth: kinetic and strain-induced roughening [31]. Kinetic roughening mainly dominant in low temperature growth as it is due to the lack of energy to cross step edges so that form multiple-level-growth, while strain-induced roughening predominantly affects high temperature strained heteroepitaxy. As we are in low temperature growth regime, kinetic roughening dominates. The nominal Sn composition in our experiment is high, which increases the total strain energy. Relaxation through stain-induced roughening becomes thermodynamically favourable when the energy cost related to increased surface area is overcome by the decrease in film strain energy due to dilatation in interplanar spacings near island peaks [31], i.e. strain enhances the overall roughening rate. In addition, the thermal activation required for strain-induced roughening can also be lowered by the local surface chemical potential gradients provided by the kinetic roughening [31]. An example is that we found similar AFM images of 274 nm Ge0.957Sn0.043 and 165 nm Ge0.939Sn0.061 grown on Ge in reference [31]. Except for the slightly improved image contrast at the hills and pits, almost no changes were observed in surface morphology for the sample annealed at 300 °C (see Figure 1(b)) compared with the as-grown surface. After annealing at 350 °C, some indistinct cross-hatch patterns (periodic surface undulations) began to show up, as seen in the bottom left corner of Figure 1(c). For samples annealed between 400 °C and 500 °C, obvious cross-hatch patterns appeared on the surface (see Figure 1(d-f)). The spacing between adjacent cross-hatch lines is around 0.5-1 μm. Cross-hatch pattern occurs when the misfit dislocation spacing is smaller than the epilayer thickness, and it has a much larger spacing than the misfit dislocation spacing [32]. In other words, the misfit dislocation spacing in the GeSn epilayer annealed at 350-500 °C should be 1-2 orders of magnitude smaller than 0.5-1 μm. Cross-hatch patterns are reported to result from the nucleation and gliding of the misfit dislocations in the {111} planes [33, 34] and are confirmed to be related to inhomogeneous strain field within the epilayer [32]. In this case, it indicates that by thermal annealing the strain can be relieved through the nucleation and gliding of the misfit dislocations, i.e. preventing the increase in threading dislocations penetrating to and degrading the crystal quality of the active GeSn layer [34]. Except for these cross-hatch patterns, the surface morphology remained stable at this annealing temperature window, i.e. 300-500 °C. Reduced roughness was observed in the samples annealed at 300-350 °C and 450-500 °C. However, the surface morphology varied significantly after annealing at 550 °C and above, as can be seen in Figure 1(g-h). 'Broken' surfaces were observed, where the perpendicular cross-hatch patterns remained in Figure 1(g), only lined-patterns stood in Figure 1(h), and the GeSn surface character (as seen in the as-grown AFM image Figure 1(a)) faded in both images with numerous black spots on the surface after annealed at 550 °C and enlarged at 600 °C. The corresponding sharp increase in surface roughness for annealing temperature of 550 and 600 °C can be seen in Figure 1(g) and (h). Meanwhile, milky spots on the surface can be seen with the naked eye for these two samples, with a higher density for the sample annealed at 600 °C. These investigations are in good agreement with others' works on GeSn annealing with similar Sn content, where the significant changes in surface morphology were confirmed to be a result of Sn out-diffusion and precipitation on the surface [18, 19]. The black spots in AFM images were believed to be the holes created by Sn out-diffusion. To understand the dynamics of the changing strain state corresponding to the occurrence and disappearance of cross-hatch patterns and the broken surfaces, HRXRD (004) symmetric scans and RSMs were applied.

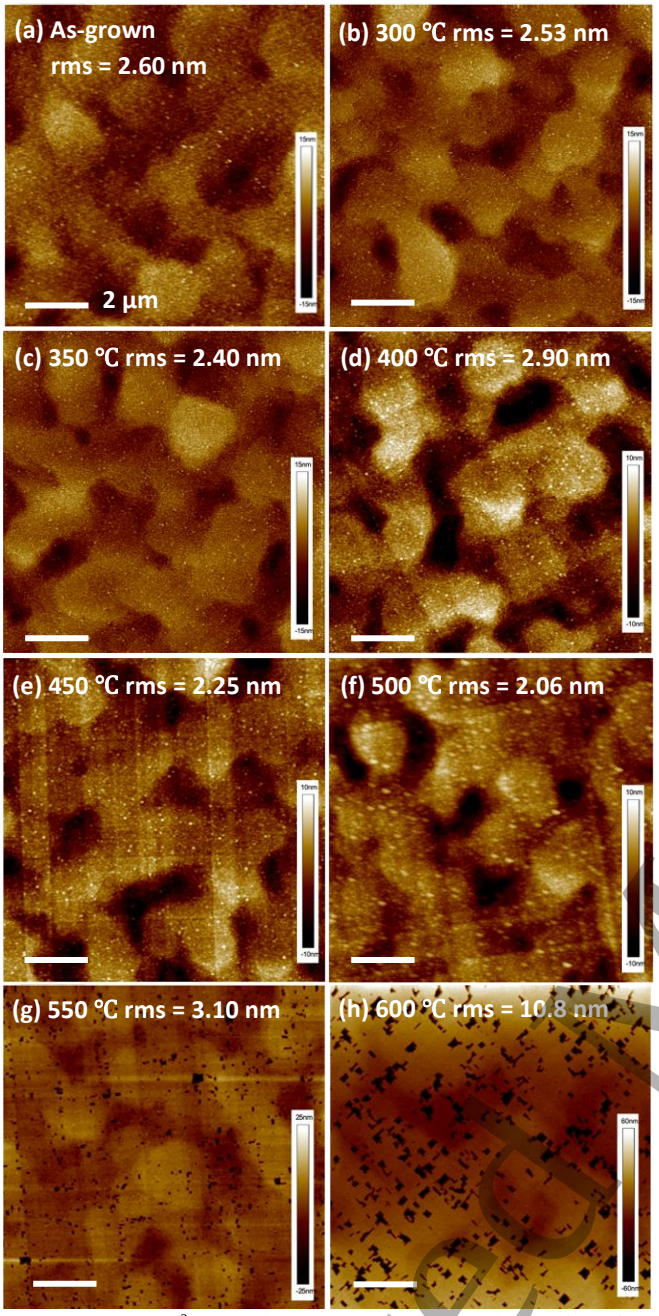

Figure 1. 10 × 10 µm^2 Atomic force microscopy images of the surface of (a) as-grown GeSn with nominal 8% Sn and (b-h) after thermal treatment at various temperatures between 300-600 °C. Root-mean-square roughness is shown in each image. Scale bars are the same of 2 µm as labelled in (a).

3.2 Strain state

First, HRXRD symmetric omega-2theta scans around (004) lattice plane were applied to probe the growth-direction lattice

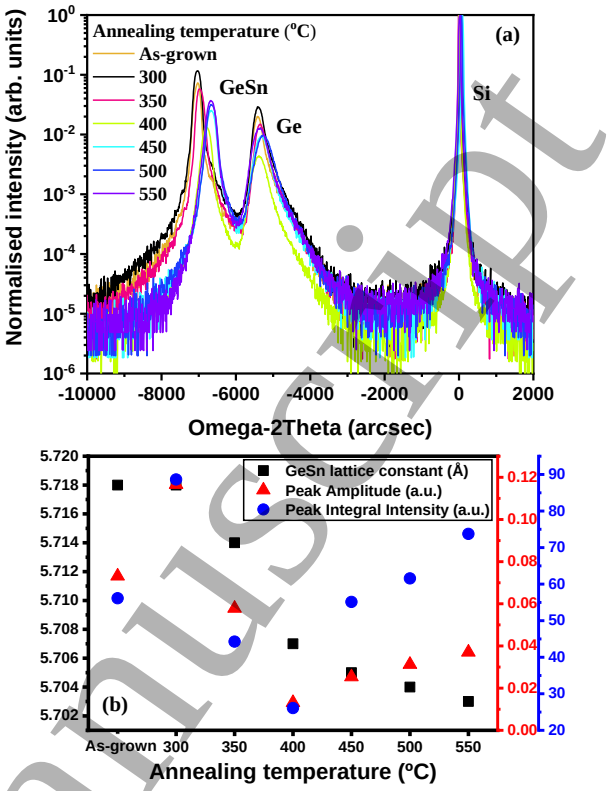

Figure 2(a) X-ray diffraction omega-2theta scans of GeSn as-grown and annealed at various temperatures. (b) Growth-direction GeSn lattice constant (black squares), peak amplitude (red triangles) and peak integral intensity (blue dots) change with annealing temperature, extracted from (a).

change. Three distinct peaks corresponding to GeSn, Ge and Si are labelled, as can be seen in Figure 2(a). The peak amplitude was normalised to show the effect of thermal annealing, and all the spectra were referenced to Si peak. Sharper and stronger diffraction peaks of GeSn than Ge can be clearly observed, indicating higher crystallinity and larger thickness of the GeSn film. This observation is in contrast with studies on GeSn thermal annealing where thick Ge buffer layers, i.e. few microns are applied to ensure full relaxation of Ge [15, 16]. The obvious asymmetric shape of the Ge peak shown in all samples is believed to be a result of Ge-Si interdiffusion. Peak amplitude, peak integral intensity and GeSn lattice constant of each sample annealed at different temperatures were also extracted and presented in Figure 2(b). The GeSn peak position of the sample annealed at 300 °C did not shift compared with the as-grown sample, but the signal intensity significantly increased (by 58%, calculated from both peak amplitude and peak integral intensity), indicating structural stability and improved crystallinity at this annealing temperature. For samples annealed at 350-450 °C the GeSn peaks shift continuously to larger values, corresponding to

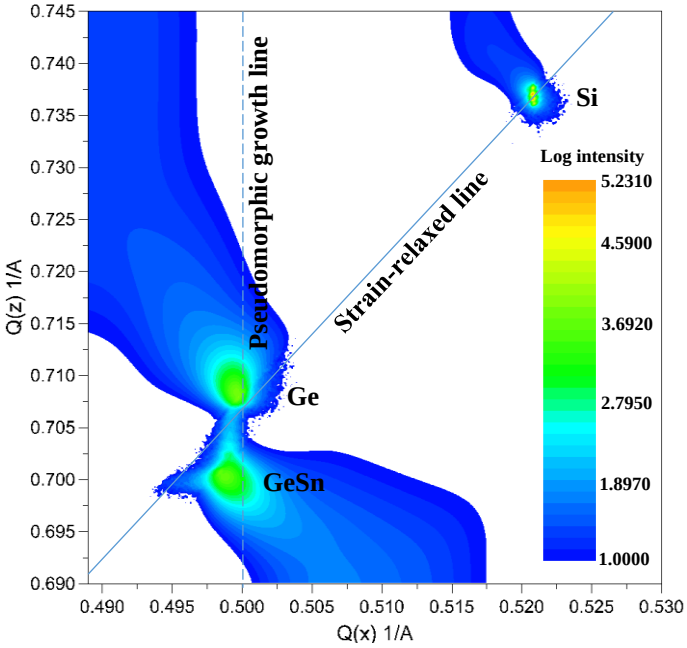

Figure 3. X-ray diffraction reciprocal space map around (224) lattice plane of as-grown GeSn. Form this map, in-plane (a_i) and growth direction (a_g) lattice constants can be calcualted by $a_i = 2\sqrt{2}/Q(x)$, $a_g = 4/Q(z)$.

smaller growth-direction lattice parameters. The peak amplitude and peak integral intensity decrease with higher annealing temperature at 350 and 400 °C, especially at 400 °C, indicating slightly degraded crystal quality. However, after the annealing temperature reaches 450 °C, the peak amplitude and peak integral intensity slowly recovered to levels half of the as-grown sample. The signal of the sample annealed at 600 °C was completely lost presumably because metallic β-Sn clusters on the surface absorbed the x-rays [29-30, 35-36]. The two different phases of solid Sn precipitates semiconductor phase α-Sn with diamond structure and metallic phase β-Sn with body-centred tetragonal unit cell have an allotropic phase transition temperature of as low as 13.5 °C [30]. α-Sn is stable below this allotropic phase transition temperature while β-Sn phase is stable above this point. Although the transition between α-Sn and β-Sn may also be affected by pressure and interface effects so that α-Sn can persist up to e.g. 200 °C in $Si_{0.95}Sn_{0.05}$ [29], in our experiment, the 600 °C annealing is too high for α-Sn precipitates to sustain.

A clear trend of the decreased lattice parameters in GeSn layers with raising temperature is observed. At first, we considered it to be the effect of Sn segregation during thermal treatment. However, that does not explain the GeSn lattice constant decrease when the annealing temperatures are below 550 °C, especially the sharp drop between 350 and 400 °C. As indicated by the AFM images, those significant changes to the crystal lattice only happened at 550-600 °C annealing temperatures. Moreover, milky spots seen on the wafer surface were observed after high temperature annealing at 550 and 600 °C. To gain further knowledge of the annealed samples

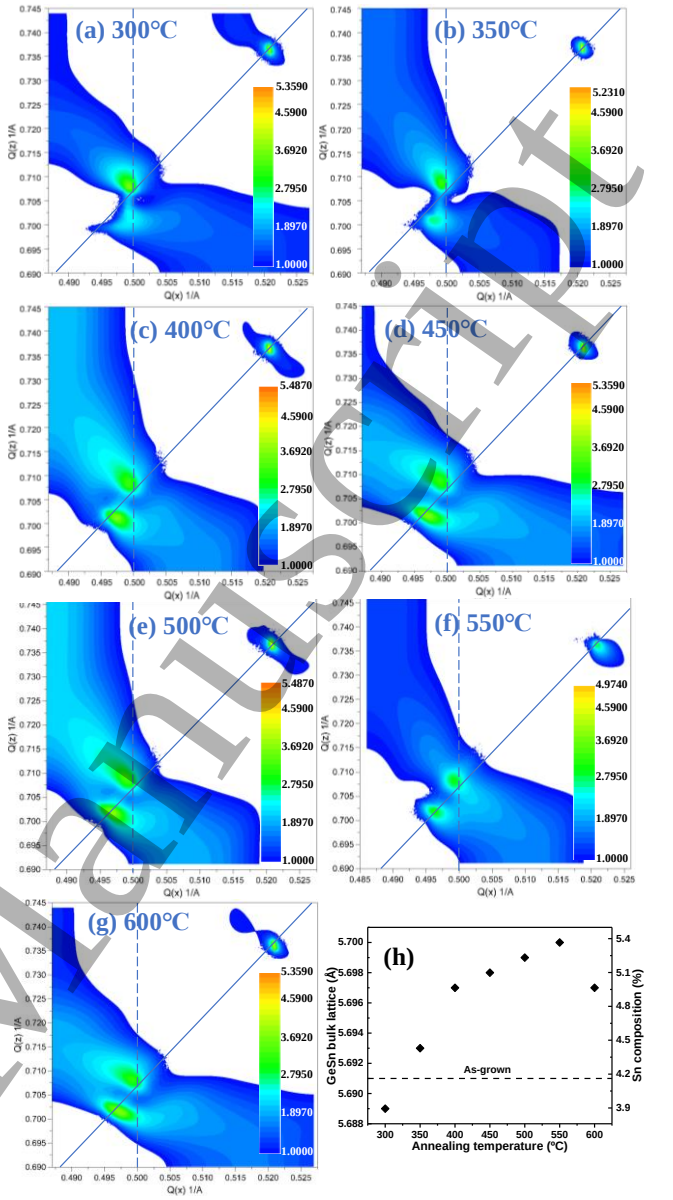

Figure 4(a-g) Reciprocal space maps around (224) reciprocal lattice point of GeSn samples annealed at different temperatures between 300-600 °C. All the maps were set at the same log signal intensity (from 1.0000 to 6.0000) to compare the crystal quality via the mosaic spread. The scale bars show the log intensity range of the maps. (h) Calculated GeSn bulk lattice constants with increasing annealing temperature.

in terms of Sn composition, strain state and crystalline quality, RSMs around (224) lattice plane were adopted as they provide the most amount of information.

RSMs can supply strain state information about the epilayers intuitively through the angle between epilayer diffraction peak and pseudomorphic-growth line (or strain-relaxed line). It can also be translated quantitatively to the in-plane and growth direction lattice parameters. The RSM around asymmetric (224) reflection of the as-grown GeSn sample is shown in Figure 3. Three peaks corresponding to Si, Ge and GeSn have been labelled at the right-hand side of each peak. One vertical dotted pseudomorphic-growth line

indicating a fully strained crystal lattice, where the epilayer has the same lattice parameter with the Ge layer underneath, and one diagonal solid strain-relaxed line suggesting a fully-relaxed lattice with cubic structure are marked. From Figure 3 it can be intuitively observed that the GeSn epilayer in the as-grown sample is relaxed to some extend as the GeSn peak deviates from the pseudomorphic growth line. This is due to the 500 nm GeSn layer thickness has far-exceeded the critical thickness for the onset of strain relaxation.

The impacts of different thermal annealing temperatures between 300-600 °C to GeSn layer are presented in the RSM measurements of Figure 4(a-g). All the peak intensities of the RSMs in Figure 4(a-g) were set to the same range (log intensity from 1.0000 to 6.0000) so that a comparison of the peak profile could be presented. The peak profile can be defined as the coloured area of each peak. After thermal annealing at 300 °C the GeSn peak is close to the pseudomorphic-growth line, indicating large compressive strain within the GeSn epilayer, as shown in Figure 4(a). In Figure 4(b) when the annealing temperature was increased to 350 °C, the GeSn peak started to move towards the strain-relaxed line. Improved crystallinity of GeSn was also observed as indicated by the shrunken peak profile. The peak positions of GeSn keep moving steadily to the strain-relaxed line after annealing at 400 and 450 °C, as shown in Figure 4(c) and (d), respectively. In summary, an increase of strain relaxation with rising annealing temperature between 350-450 °C was observed, and nearly full degree of relaxation was achieved after the annealing temperature reaches 450 °C. GeSn peaks sit around the strain-relaxed line for samples annealed at 450-600 °C (see Figure 4(d-g). However, another clear observation is that the peak profiles of Ge and GeSn are significantly enlarged upon annealing temperature hitting 400 °C. These enlarged profiles are accompanied by the strain relaxation processes as the GeSn peaks shift towards the strain-relaxed line, proving the onset of strain relaxation induced by thermal annealing and are also consistent with the observations in AFM cross-hatch results. This phenomenon is recognised as a mosaic spread process where the peak profiles become enlarged because of the slight misorientations of the crystal lattice. The in-plane (a_i) and growth-direction (a_g) lattice parameters of Ge and GeSn were extracted from RSMs, and the bulk lattice constant (a_b) of GeSn was calculated considering the Poisson ratio (μ = 0.28, the Poisson ratio of Ge) by [19]:

$$a_b = \frac{a_g + 2a_i\mu}{1 + 2\mu}$$

The bulk GeSn lattice constants and corresponding Sn composition calculated by applying Vegard's law are shown in Figure 4(h). In contrast with the lattice constants decreasing with rising annealing temperature obtained from symmetric (004) scans, there is an upward trend of GeSn bulk lattice constants calculated from RSMs, except at 300 °C and 600 °C. The shift of GeSn lattice constant towards Ge at 300 °C annealing is counter-intuitive, and the increase of GeSn lattice constant at 550 °C is also unexpected as Sn out-diffusion has happened at this temperature as inferred from the AFM images. To provide possible explanations to these observations, in-plane and growth direction lattice constants of Ge and GeSn are summarised in Figure 5(a-b). It can be seen from Figure 5(a) that the 250 nm Ge buffer is under tetragonal tensile strain both before and after thermal annealing. The Ge in-plane lattice constant kept growing while the growth-direction parameter shrank correspondingly despite some fluctuations under thermal annealing between 300-500 °C, until annealing temperature reached 550 °C breaking this trend. The most pronounced Ge lattice parameter changes happened at 300 °C and 550 °C. Correspondingly, the GeSn epilayer is under tetragonal compressive strain before and throughout the thermal processing as shown in Figure 5(b). The GeSn in-plane lattice constants keep growing with higher annealing temperatures between 350 and 550 °C while the growth-direction lattice constants are rather stable. 300 and 600 °C annealing caused significant in-plane lattice constant shrinkage of GeSn. At 300 °C the Ge in-plane lattice constant increased the most, indicating enlarged in-plane strain, which we suspect to be a result of the interaction between GeSn and the underlying Ge, as 300 °C annealing should not make significant difference to Ge, but it will change the behaviour of GeSn, especially the Sn diffusion. This provides some hints to explain the decreased lattice constant of GeSn under 300 °C annealing based on the postulation that the thermal energy stored in GeSn layer was consumed by inducing strain in the underlying Ge. At 550 °C the tensile-strained Ge turned to relax close to its bulk value. This observation is in line with our expectations and can be explained by the decreased GeSn lattice at the GeSn/Ge interface inducing less tensile strain on Ge. As for the increased in-plane GeSn lattice constant at 550 °C, one possibility is that the Sn out-diffusion left many vacancies at the GeSn lattice, the local strain was reduced by the combination of Sn atoms with vacancies [17], leading to expanded lattice constants. The increase in the total change of lattice constant from the sum of Ge and GeSn both in in-plane- and growth-direction and the raised strain relaxation at 550 °C, as presented in Figure 5(c) and (d), respectively, support this assumption. Another important observation in our experiments is that the Sn segregation process under high temperature annealing, i.e. 550-600 °C is unequivocally different from the results of the pioneering work in this topic where a sudden Sn segregation inducing a stable low-Sn-composition (1%) phase within temperature change of around 20 °C after reaching the critical annealing temperature was observed for pre-relaxed GeSn [16]. From our results, the Sn segregation process is comparatively slow, with a final Sn composition of 5%. Indeed, our results agreed with earlier

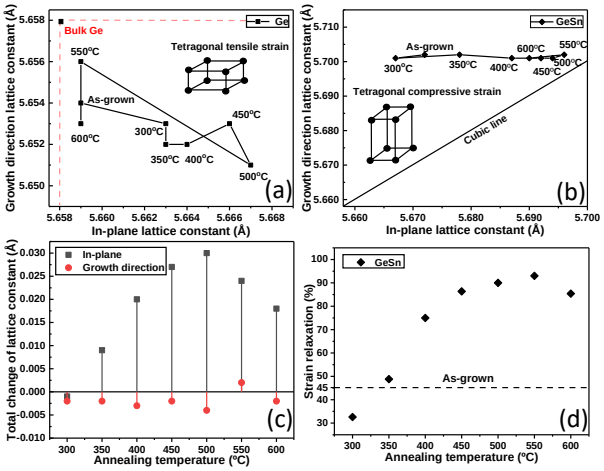

Figure 5. In-plane and growth direction lattice constants of (a) Ge buffer and (b) GeSn under different annealing temperatures. (c) A total change of lattice constant in Å. (d) Strain relaxation with annealing temperature measured from RSMs.

work on the gradual Sn segregation process, and they reached a final Sn composition of 4.1% [19]. These contrasting behaviours were considered to derive from different growth conditions, i.e. chemical vapour deposition (CVD) or MBE growth as the growth temperature, and dynamics were different, underneath buffer layers in terms of thicknesses and defect conditions [15] and annealing processes where ex-situ rapid thermal annealing or in-situ gently-ramped annealing were adopted.

4. Conclusion

We applied ex-situ rapid thermal processing to 500 nm nominal 8% Sn composition GeSn samples grown on 250 nm Ge on Si (001) substrate by MBE at temperatures between 300-600 °C for 5 minutes each, aiming at finding the feasibility of using this annealed high-Sn-content GeSn layer as a buffer for GeSn laser devices. It was found from AFM images that the surface was slightly improved at 300-350 °C, 450-500 °C annealing, while the featured-GeSn surface was destroyed after annealing temperature reached 550 °C, indicating Sn-segregation process. Strain states within GeSn layer were probed quantitatively and qualitatively by HRXRD. It was found that below 600°C with increasing annealing temperature, the strain relaxation increased steadily, and peaked at 550 °C of 93%, despite the counter-intuitive decrease in 300 °C, which was considered to result from the interaction between GeSn and the underneath Ge layer. However, different behaviours with others' work for 'pre-relaxed' GeSn layer where they reported sudden Sn segregation and a sharp transition to a low-Sn-composition phase on critical annealing temperature were observed in our experiments, relatively gradual reduction in lattice constant after annealing temperature reaching 550 °C and a final Sn composition of 5% was found. Our results show that although the thermal stability of GeSn varies significantly with Sn composition, strain state, underneath buffer and crystal quality, thick annealed GeSn layers can be used as buffer layers for GeSn-based optoelectronic devices to provide large extent of strain relaxation while maintaining crystal quality upon delicate selection of annealing conditions. An annealing temperature of 500 °C applied to a 500 nm GeSn buffer of nominal 8% Sn was the best fit in our case to provide matched-lattice parameters, strain relaxation and good crystal quality without Sn segregation for higher Sn composition GeSn active layer.

Acknowledgements

UK Engineering and Physical Sciences Research Council – EPSRC under Grant EP/P006973/1 and EPSRC National Epitaxy Facility, and Royal Academy of Engineering (RF201617/16/28).

References

[1] Eales T D, Marko I P, Schulz S, O'Halloran E, Ghetmiri S, Du W, Zhou Y, Yu S Q, Margetis J, Tolle J, O'Reilly E P and Sweeney S J 2019 $Ge_{1-x}Sn_x$ alloys: Consequences of band mixing effects for the evolution of the band gap Γ-character with Sn concentration *Sci. Rep.* **9** 1–10

[2] Jenkins D W and Dow J D 1987 Electronic properties of metastable Ge_xSn_{1-x} alloys *Phys. Rev. B* **36** 7994–8000

[3] Oehme M, Kostecki K, Schmid M, Oliveira F, Kasper E and Schulze J 2014 Epitaxial growth of strained and unstrained GeSn alloys up to 25% Sn *Thin Solid Films* **557** 169–72

[4] Nakamura M, Shimura Y, Takeuchi S, Nakatsuka O and Zaima S 2012 Growth of $Ge_{1-x}Sn_x$ heteroepitaxial layers with very high Sn contents on InP(001) substrates *Thin Solid Films* **520** 3201–5

[5] Brownlee L D 1950 Lattice constant of grey tin *Nature* **166** 482

[6] Von Den Driesch N, Stange D, Wirths S, Mussler G, Holländer B, Ikonic Z, Hartmann J M, Stoica T, Mantl S, Grützmacher D and Buca D 2015 Direct Bandgap Group IV Epitaxy on Si for Laser Applications *Chem. Mater.* **27** 4693–702

[7] Rainko D, Ikonic Z, Elbaz A, von den Driesch N, Stange D, Herth E, Boucaud P, El Kurdi M, Grützmacher D and Buca D 2019 Impact of tensile strain on low Sn content GeSn lasing *Sci. Rep.* **9** 1–9

[8] Dou W, Benamara M, Mosleh A, Margetis J, Grant P, Zhou Y, Al-Kabi S, Du W, Tolle J, Li B, Mortazavi M and Yu S Q 2018 Investigation of GeSn Strain Relaxation and Spontaneous Composition Gradient for Low-Defect and High-Sn Alloy Growth *Sci. Rep.* **8** 1–11

[9] Grant P C, Margetis J, Zhou Y, Dou W, Abernathy G, Kuchuk A, Du W, Li B, Tolle J, Liu J, Sun G, Soref R A, Mortazavi M and Yu S Q 2018 Direct bandgap type-I GeSn/GeSn quantum well on a GeSn- and Ge- buffered Si substrate *AIP Adv.* **8**

[10] Dou W, Zhou Y, Margetis J, Ghetmiri S A, Al-Kabi S, Du W, Liu J, Sun G, Soref R A, Tolle J, Li B, Mortazavi M and Yu S-Q 2018 Optically pumped lasing at 3 μm from compositionally graded GeSn with tin up to 22.3% *Opt. Lett.* **43** 4558

[11] Zhou Y, Dou W, Du W, Ojo S, Tran H, Ghetmiri S A, Liu J, Sun G, Soref R, Margetis J, Tolle J, Li B, Chen Z, Mortazavi M and Yu S Q 2019 Optically Pumped GeSn Lasers Operating at 270 K with Broad Waveguide Structures on Si ACS Photonics 6 1434–41

[12] Chrétien J, Pauc N, Armand Pilon F, Bertrand M, Thai Q M, Casiez L, Bernier N, Dansas H, Gergaud P, Delamadeleine E, Khazaka R, Sigg H, Faist J, Chelnokov A, Reboud V, Hartmann J M and Calvo V 2019 GeSn Lasers Covering a Wide Wavelength Range Thanks to Uniaxial Tensile Strain ACS Photonics 6 2462–9

[13] Stange D, Wirths S, Geiger R, Schulte-Braucks C, Marzban B, Driesch N V Den, Mussler G, Zabel T, Stoica T, Hartmann J M, Mantl S, Ikonic Z, Grützmacher D, Sigg H, Witzens J and Buca D 2016 Optically Pumped GeSn Microdisk Lasers on Si ACS Photonics 3 1279–85

[14] Elbaz A, Buca D, von den Driesch N, Pantzas K, Patriarche G, Zerounian N, Herth E, Checoury X, Sauvage S, Sagnes I, Foti A, Ossikovski R, Hartmann J M, Boeuf F, Ikonic Z, Boucaud P, Grützmacher D and El Kurdi M 2020 Ultra-low-threshold continuous-wave and pulsed lasing in tensile-strained GeSn alloys Nat. Photonics

[15] von den Driesch N, Wirths S, Troitsch R, Mussler G, Breuer U, Moutanabbir O, Grützmacher D and Buca D 2020 Thermally activated diffusion and lattice relaxation in (Si)GeSn materials Phys. Rev. Mater. 4 4–9

[16] Zaumseil P, Hou Y, Schubert M A, Von Den Driesch N, Stange D, Rainko D, Virgilio M, Buca D and Capellini G 2018 The thermal stability of epitaxial GeSn layers APL Mater. 6

[17] Zaima S, Nakatsuka O, Taoka N, Kurosawa M, Takeuchi W, Sakashita M, Zaima S, Nakatsuka O and Taoka N 2015 Growth and applications of GeSn-related group-IV semiconductor materials Growth and applications of GeSn-related group-IV semiconductor materials Sci. Technol. Adv. Mater. 16 43502

[18] Zhang Z P, Song Y X, Li Y Y, Wu X Y, Zhu Z Y S, Han Y, Zhang L Y, Huang H and Wang S M 2017 Effect of thermal annealing on structural properties of GeSn thin films grown by molecular beam epitaxy AIP Adv. 7

[19] Li H, Cui Y X, Wu K Y, Tseng W K, Cheng H H and Chen H 2013 Strain relaxation and Sn segregation in GeSn epilayers under thermal treatment Appl. Phys. Lett. 102

[20] Chang C, Li H, Chen T P, Tseng W K, Cheng H, Ko C T, Hsieh C Y, Chen M J and Sun G 2015 The strain dependence of $Ge_{1-x}Sn_x$ (x = 0.083) Raman shift Thin Solid Films 593 40–3

[21] Wang W, Li L, Zhou Q, Pan J, Zhang Z, Tok E S and Yeo Y C 2014 Tin surface segregation, desorption, and island formation during post-growth annealing of strained epitaxial $Ge_{1-x}Sn_x$ layer on Ge (0 0 1) substrate Appl. Surf. Sci. 321 240–4

[22] Gassenq A, Milord L, Aubin J, Pauc N, Guilloy K, Rothman J, Rouchon D, Chelnokov A, Hartmann J M, Reboud V and Calvo V 2017 Raman spectral shift versus strain and composition in GeSn layers with 6%-15% Sn content Appl. Phys. Lett. 110

[23] Lei D, Lee K H, Bao S, Wang W, Masudy-Panah S, Tan C S, Tok E S, Gong X and Yeo Y C 2017 Thermal stability of germanium-tin (GeSn) fins Appl. Phys. Lett. 111

[24] Taoka N, Capellini G, Schlykow V, Montanari M, Zaumseil P, Nakatsuka O, Zaima S and Schroeder T 2017 Electrical and optical properties improvement of GeSn layers formed at high temperature under well-controlled Sn migration Mater. Sci. Semicond. Process. 70 139–44

[25] Zhang D, Liao Y, Li J, Wen T, Jin L, Wang X and Kolodzey J 2016 Effect of in-situ annealing on the structural and optical properties of GeSn films grown by MBE J. Alloys Compd. 684 643–8

[26] Yang J, Jurczak P, Cui F, Li K, Tang M, Billiald L, Beanland R, Sanchez A M and Liu H 2019 Thin Ge buffer layer on silicon for integration of III-V on silicon *J. Cryst. Growth* **514** 109–13

[27] Gencarelli F, Vincent B, Demeulemeester J, Vantomme A, Moussa A, Franquet A, Kumar A, Bender H, Meersschaut J, Vandervorst W, Loo R, Caymax M, Temst K and Heyns M 2013 Crystalline Properties and Strain Relaxation Mechanism of CVD Grown GeSn *ECS J. Solid State Sci. Technol.* **2** P134–7

[28] Aubin J, Hartmann J M, Gassenq A, Milord L, Pauc N, Reboud V and Calvo V 2017 Impact of thickness on the structural properties of high tin content GeSn layers *J. Cryst. Growth* **473** 20–7

[29] Fyhn M F, Chevallier J, Larsen A N, Feidenhans'l R and Seibt M 1999 α-Sn and β-Sn precipitates in annealed epitaxial $Si_{0.95}Sn_{0.05}$ *Phys. Rev. B - Condens. Matter Mater. Phys.* **60** 5770–7

[30] Pukite P, Iyer S and Angeles L 1989 Molecular beam epitaxy of metastable, diamond structure Sn_xGe_{1-x} alloys *Appl. Phys. Lett.* **54**

[31] Bratland K A, Foo Y L, Spila T, Seo H S, Haasch R T, Desjardins P and Greene J E 2005 Sn-mediated Ge/Ge(001) growth by low-temperature molecular-beam epitaxy: Surface smoothening and enhanced epitaxial thickness *J. Appl. Phys.* **97**

[32] Fitzgerald E A 1992 Relaxed Ge_xSi_{1-x} structures for III–V integration with Si and high mobility two-dimensional electron gases in Si *J. Vac. Sci. Technol. B Microelectron. Nanom. Struct.* **10** 1807

[33] Hartmann J M, Abbadie A, Cherkashin N, Grampeix H and Clavelier L 2009 Epitaxial growth of Ge thick layers on nominal and 6° off Si(0 0 1); Ge surface passivation by Si *Semicond. Sci. Technol.* **24**

[34] Assali S, Nicolas J and Moutanabbir O 2019 Enhanced Sn incorporation in GeSn epitaxial semiconductors via strain relaxation *J. Appl. Phys.* **125**

[35] Asom M T, Kortan A R, Kimerling L C and Farrow R C 1989 Structure and stability of metastable α-Sn *Appl. Phys. Lett.* **55** 1439–41

[36] Tu L W, Wong G K and Ketterson J B 1989 Growth of n-type heteroepitaxial films of gray tin on (001) CdTe by molecular beam epitaxy *Appl. Phys. Lett.* 54 1010–2

[37] Wang W, Dong Y, Zhou Q, Tok E S and Yeo Y C 2016 Germanium-tin interdiffusion in strained Ge/GeSn multiple-quantum-well structure *J. Phys. D. Appl. Phys.* **49**

[38] Zhang Z P, Song Y X, Zhu Z Y S, Han Y, Chen Q M, Li Y Y, Zhang L Y and Wang S M 2017 Structural properties of GeSn thin films grown by molecular beam epitaxy *AIP Adv.* **7**

[39] Assali S, Nicolas J, Mukherjee S, Dijkstra A and Moutanabbir O 2018 Atomically uniform Sn-rich GeSn

semiconductors with 3.0-3.5 μ m room-temperature optical emission *Appl. Phys. Lett.* **112** 1–6

[40] Li H, Chang C, Chen T P, Cheng H H, Shi Z W and Chen H 2014 Characteristics of Sn segregation in Ge/GeSn heterostructures *Appl. Phys. Lett.* **105** 1–4